Engineering Lessons from the 28 September 2018 Indonesian Tsunami: Scouring Mechanisms and Effects on Infrastructure

Clemens Krautwald, M.Sc.[1]*; Jacob Stolle, Ph.D.[2]; Ian Robertson, Ph.D., S.E.[3], Hendra Achiari, Dr.Eng.[4], Takahito Mikami, Dr.Eng.[5], Ryota Nakamura, Ph.D.[6], Tomoyuki Takabatake, Ph.D.[7], Yuta Nishida[8], Tomoya Shibayama, Ph.D.[9], Miguel Esteban, Ph.D.[10], Nils Goseberg, Dr.Eng.[11], Ioan Nistor, Ph.D.[12].

[1] Research Associate, Department of Architecture, Civil Engineering and Environmental Sciences, TU Braunschweig, Beethovenstr. 51a, 38106, Braunschweig, Germany, E-Mail: c.krautwald@tu-braunschweig.de

[2] Assistant Professor, Eau Terre Environment, INRS, 490, Rue de la Couronne, G1K 9A9, Québec, Canada, E-Mail: jacob.stolle@ete.inrs.ca

[3] Professor of Civil and Environmental Engineering, Department of Civil and Environmental Engineering, University of Hawaii at Manoa, 2540 Dole St, 96822, Hawaii, USA, E-Mail: ianrob@hawaii.edu

[4] Assistant Professor, Faculty of Civil and Environmental Engineering, Institut Teknologi Bandung, Jl. Ganesa No.10, Lb. Siliwangi, Kecamatan Coblong, Kota Bandung, Jawa Barat 40132, Indonesia, E-Mail: achiarihendra@gmail.com

[5] Associate Professor, Department of Urban and Civil Engineering, Tokyo City University, 1 Chome-28-1 Tamazutsumi, Setagaya City, Tokyo, 158-0087, Japan, E-Mail: tmikami@tcu.ac.jp

[6] Associate Professor, Faculty of Engineering, Niigata University, Ikarashi 2 Nocho, Nishi Ward, Niigata, 950-2102, Japan, E-Mail: ryota_nakamura617@yahoo.co.jp

[7] Assistant Professor, Department of Civil and Environmental Engineering, Waseda University, 4-1 Okubo 3, Shinjuku-ku, Tokyo, 169-8555, Japan, E-Mail: tomoyuki.taka.8821@gmail.com

[8] Research Assistant, Department of Civil and Environmental Engineering, Waseda University, 4-1 Okubo 3, Shinjuku-ku, Tokyo, 169-8555, Japan, E-Mail: yuta325@ruri.waseda.jp

[9] Professor, Department of Civil and Environmental Engineering, Waseda University, 4-1 Okubo 3, Shinjuku-ku, Tokyo, 169-8555, Japan, E-Mail: shibayama@waseda.jp

[10] Professor, Department of Civil and Environmental Engineering, Waseda University, 4-1 Okubo 3, Shinjuku-ku, Tokyo, 169-8555, Japan, E-Mail: esteban.fagan@gmail.com

[11] Professor, Department of Architecture, Civil Engineering and Environmental Sciences, TU Braunschweig, Beethovenstr. 51a, 38106, Braunschweig, Germany, E-Mail: n.goseberg@tu-braunschweig.de

[12] Professor, Department of Civil Engineering, University of Ottawa, 115 Séraphin-Marion, Room HGN215, Ottawa, K1N 6N5, Ontario, Canada, E-Mail: inistor@uottawa.ca

** Corresponding author: Clemens Krautwald, ORCiD: 0000-0001-8928-1352*

Engineering Lessons from the 28 September 2018 Indonesian Tsunami: Scouring Mechanisms and Effects on Infrastructure

The 28th of September 2018 earthquake and tsunami north of Palu, Indonesia, attracted widespread interest from the scientific community due to the unusually large tsunami which occurred after a strike slip earthquake with a relatively small moment magnitude (M_W = 7.5). To understand the structural performance of buildings and infrastructure under hydrodynamic loads and its associated effects the authors conducted field surveys of Palu City. Light wooden frame constructions and masonry infill walls were common in the area, some of which were severely damaged by the earthquake and tsunami. Reinforced concrete structures remained predominantly intact, though suffered soil-related issues such as scour around rigid building members. Local structural failures caused by the loss of supporting soil were also observed during the field survey, resulting in an overall reduction in the stability of the inspected structures. Based on the observations made, knowledge gaps and research needs concerning coastal and structural scouring are discussed. These are tied into the latest community research activities and put in the context of the published tsunami design standard in Chapter 6 of ASCE 7-16 (2017).

Keywords: Palu tsunami; field survey; scouring mechanisms; hydrodynamic forces; coastal engineering; engineering lessons

1 Introduction

Palu City is situated on the southern shore of a bay on the northwest side of the Central Sulawesi province of Indonesia. The bay has a length of about 30 km, widths of between 6 and 7 km and depths of up to 700 m (Takagi et al. 2019). The province is in a region that is vulnerable to earthquakes that is surrounded by multiple subduction zones and faults, including the active Palu-Koro strike-slip fault, which traverses Palu City (Bahar et al. 1997). Prasetya et al. (2001) reported two tsunami events originating from this fault in Palu Bay, the first of which occurred on December 1st 1927 and the second one on August 14th 1968. The moment magnitudes of these earthquake events were relatively small: $M_W = 6.3$ in 1927 and $M_W = 7.4$ in 1968. However, these events triggered tsunami wave heights of 15 m and 10 m in 1927 and 1968, respectively (Prasetya et al. 2001). Both tsunamis were triggered by a strike-slip tectonic rupture motion, which usually does not favor the generation of such phenomena (Papadopoulos 2016), demonstrating that tectonic rupture motions and resulting tsunami magnitudes sometimes diverge.

A strike-slip earthquake with a $M_W = 7.5$ occurred near Palu City on the 28th of September 2018, at 18:02:43 local time. The epicentre was located approximately 100 km north east of the city at a depth of 20 km (USGS 2018). Tsunami waves were triggered and were reported to have unusually high inundation depths and rapid arrival times, despite the relatively modest magnitude and tectonic motion of the earthquake. Aránguiz et al. (2019) numerically analysed possible secondary landslide generation mechanisms using measured bathymetry data and visual observation of possible locations of underwater landmass movements. Numerical simulations were performed to assess the sequence of this tsunami event, which indicated that a superposition of the seismic event and waves generated by a series of landslides led to the tsunami impact in Palu City. Sassa and Takagawa (2018), stressed that liquefaction due to the earthquake was observed not only inland but also along the coastline. Therefore, the submarine landslides were characterized as liquefied gravity flows. Overall, the scientific community is in good agreement that coastal landslides played an important contribution to the generation mechanism of this tsunami phenomenon and found evidence for them at 6 (Arikawa et al. 2018), 12 (Omira et al. 2019, Widiyanto et al. 2019) and 13 (Robertson et al. 2019) locations. Additionally, energy focusing due to the offshore bathymetry and shape of Palu Bay contributed to the high wave heights near Palu City (Ulrich et al. 2019).

A reconnaissance team led by the Waseda University, Japan, consisting of members from Japan, USA, Indonesia, Canada and Germany, visited Palu Bay from the 27th to 31st of October 2018. The objectives of this post-tsunami survey were to investigate the tsunami generation mechanisms, to collect data concerning the flooding extent, and to reveal knowledge gaps in tsunami-driven structural failure modes. The present work focuses on the hydrodynamic loading and scouring around structures, comparing them with recent tsunami design practices. The ultimate goal is to provide insights that tie knowledge from the post-hazard survey to current design standards, and to specifically elucidate relevant knowledge gaps pertaining to soil instability uncovered during the literature review, field campaign, and analysis.

The paper is structured as follows: Section 2 describes the current state-of-the-art in tsunami-resistant design, including uplift forces on structures, soil stability, and the geotechnical considerations. This literature review is specifically provided to lay the basis to interpret the observations made during the post-disaster survey. Section 3 focuses on the methodology of the field survey and the general characteristics of the tsunami event and site-specific structures. Structural failures observed during the post-tsunami survey are categorized according to uplift forces, soil stability and scour-induced structural failures, which are presented in Section 4. The engineering lessons learned during the post-tsunami survey are summarized in Section 5. Conclusions are presented Section 6.

2 Review of Relevant Tsunami-Resistant Design Aspects

2.1 Uplift Forces

ASCE 7-16 Chapter 6 (2017) distinguishes between hydrostatic and hydrodynamic uplift forces (see Figure 1). Hydrostatic uplift forces are mainly induced by buoyancy, which depends on the displaced water volume by structural components, enclosed air-tight volumes below the inundation level, floor soffits and structural slabs. Entrapped air under girders should also be considered in the displaced water volume. Structural components which are expected to collapse during inundation decrease the buoyancy forces as result of the increased air outflow (ASCE 7-16 2017). Hydrodynamic forces are generally divided into drag forces, hydrodynamic uplift forces and impulsive forces (Palermo et al. 2013).

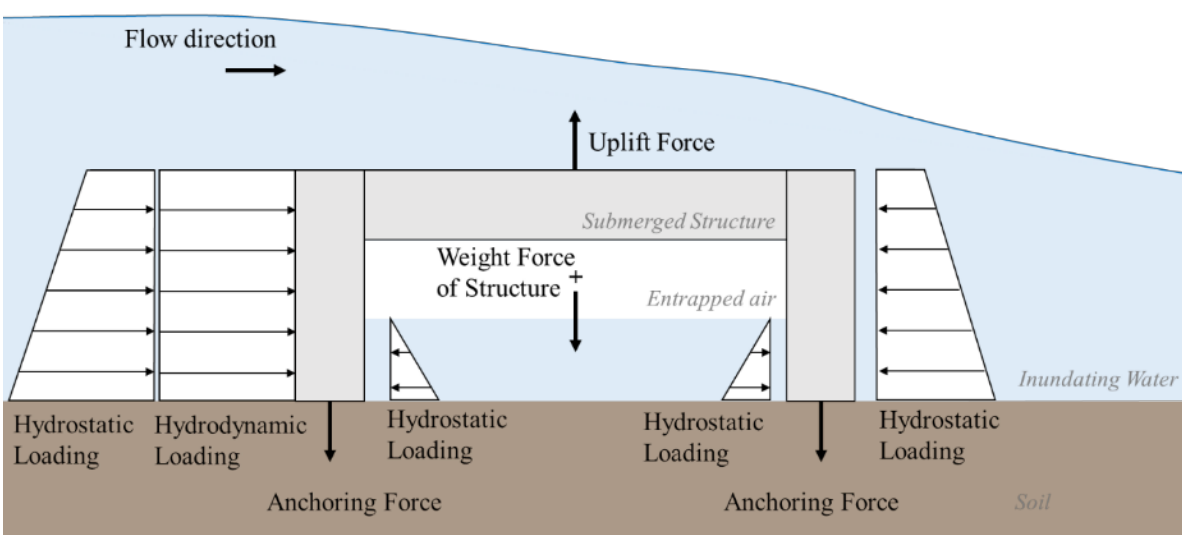

Figure 1: Vertical forces and horizontal pressure distributions on a submerged structure during tsunami inundation.

Additional uplift forces occur when a tsunami inundates a structure with entrapped air in it. Seiffert et al. (2014) and Seiffert et al. (2015) investigated nonlinear wave loading on coastal bridge decks, either using simplified plates only or including girders. When waves inundate a bridge deck with girders, air can be trapped in the gap between two girders. Dynamic water motion leads to the compression of the entrapped air and to impulse pressure peaks at the bridge decks. Seiffert et al. (2015) experimentally analysed the effects of air relief openings and found a significant reduction of vertical uplift forces when large openings are present. Further, Moideen et al. (2019) built upon the experimental data to perform a parametric study on vertical impact forces with the computational fluid dynamics (CFD) model REEF3D (Bihs et al. 2016), analysing the effect of wave heights, girders spacing and depth for varying air gaps. That study confirmed higher vertical impact forces for bridge decks with girders where air can be trapped. Furthermore, vertical impact forces were found to increase for larger air gaps and for smaller girder spacing. Whereas the ASCE 7-16 Chapter 6 (2017) mentions entrapped air as a potential source of uplift force, the current version of the standard does not yet detail precise calculation methods for the impact uplift pressure on horizontal structures incorporating entrapped air. Del Zoppo et al. (2019) address the effect of tsunami-induced vertical loads, including buoyancy, on the design of reinforced concrete frame structures. The need for more in-depth prescriptions was also highlighted in a previous post-tsunami field surveys identifying the overturning failure of a four-story RC building in Onagawa City, Japan, during the 2011 Tohoku Earthquake and Tsunami as a result of combined hydrodynamic loading, buoyant forces with trapped air and pore pressure softening (Yeh et al. 2013).

2.2 Soil Stability

2.2.1 General Erosion

During foundation design of tsunami-resilient structures, soil instabilities, such as erosion and pore pressure softening, have to be considered. Erosion may take a number of forms: (a) general erosion marking a loss of land surface over large spatial extents (Dalrymple and Kriebel 2005, Shuto and Fujima 2009, Kato et al. 2012, Yeh et al. 2013, Fraser et al. 2013), (b) sustained flow scour near corners and sides around free-standing structures, with scour depth ranging from 0.5 - 4.0 m being reported by post-tsunami field surveys (Bricker et al. 2012, Tonkin et al. 2013), (c) channelized scours in between gaps of larger buildings, as reported by Yeh et al. (2013) in the city of Onagawa, Japan during the 2011 Tohoku Earthquake Tsunami, and (d) overtopping scour behind coastal line defenses such as sea walls, where overtopping jets plunging over the structures cause excessive soil erosion (Yeh et al. 2004, Kato et al. 2012, Mikami et al. 2014, Jayaratne et al. 2016). All forms of scouring listed above may, when the extreme flow event is persistent and exposes the soil to shear stresses larger than the critical shear stress, result in scouring that could eventually damage structures; only recently, guidelines and standards have started to address this important issue. According to the ASCE 7-16 Chapter 6 (2017), different load cases should include simultaneous considerations of scour, seismic liquefaction and pore pressure softening when assessing the foundation stability. Critical load cases include (a) soil saturation before tsunami inundation, (b) soil saturation during tsunami inundation and (c) cases when the area is still inundated after the tsunami (ASCE 7-16 2017).

General erosion is typically expressed in terms of the Mohr-Coulomb (Mohr 1914) or the Shields criterion (Shields 1936, Rijn 1993). Manenti et al. (2012) carried out experimental and numerical analysis of rapid water discharge to compare the practical applicability of the approaches of Mohr-Coulomb and Shields. The study determined that the Shields approach better represents sediment dynamics and to be of higher practical use, as the parameters are based on measurable physical quantities. ASCE 7-16 Chapter 6 (2017) states that general erosion shall be determined according to standard literature or models, such as the numerical software HEC-RAS (USACE 2016), which incorporates the Shields approach. The Shields parameter was originally derived for the incipient movement of sediment particles in hydraulic experiments (Shields 1936). Nowadays, the Shields parameter has been adapted and extensively used to describe sediment transport for a variety of flow conditions in marine environments (Madsen and Grant 1976, Rijn 1984, Sumer and Fredsoe 2002).

Quasi-steady flow conditions occur when the tsunami inundation motion forms an overland current during run-up and draw-down phases. Transient flow conditions with varying flow velocities and pressures happen between these two phases. Yeh and Mason (2014) modified the Shields parameter in relation to tsunami inundation to include the effect that soil is stabilized during tsunami run-up due to a positive pore pressure gradient and destabilized during draw-down when there is a negative pore pressure gradient.

More recent research questions the usability of the Shields approach when assessing the incipient motion for non-uniform sediments, wide-graded materials (where other issues such as hiding and exposure effects can be important). Hiding effects require higher shear stresses to mobilize finer sediments when coarser grains surround them, while the exposure effect qualifies the decreased resistance of coarse grains due to their unstable placement on finer sediments. Shvidchenko et al. (2001) proposed to use statistical parameters such as the relative grain size to include these effects. Further research was performed by Schendel et al. (2016) and Schendel et al. (2018) to investigate the stability of wide-graded material under unidirectional and reversing currents. Both studies emphasized that the Shields approach is insufficient to assess the erosion-stability and the average grain diameter d_{50} is insufficient to adequately represent the material characteristics.

Resistance to scour is defined by soil properties such as soil type, grain sizes, permeability and saturation, while acting forces on the soil depend on hydrodynamic parameters such as flow velocity, flow depths, directions and turbulence intensities (Francis 2006). In built-up environments, flow properties can depend on structural and topographical layouts, such as the spacing, sizes, shapes and orientation of buildings (Goseberg 2013). Results of a post-tsunami survey by Yeh et al. (2013) after the 2011 Tohoku Earthquake Tsunami indicated the flow amplifying effects of large RC buildings, leading to higher bottom shear stresses and increased sediment transport next to structures due to channelization and the formation of jets. To conclude, the physical processes leading to sediment transport and soil instabilities are complex and not entirely understood. Further research is needed to elucidate these processes and include them in current guidelines and standards such as ASCE 7-16 (2017).

2.2.2 Pore Pressure Softening

The load bearing potential of soil relies on the contact between grains. Changes in hydrostatic pressure, ground shaking, dislocations and infiltration of water, may substantially increase pore pressure and reduce ~~this~~its load bearing capacity. ~~When the pore pressure force exceeds the gravity acting on the soil, pore pressure softening occurs.~~ When the induced pore pressures exceeds the overburden weight pressure, momentary liquefaction can take place~~ liquefaction~~ (Sumer and Fredsoe 2002). This is a particular risk during the draw-down sequence of a tsunami where hydrostatic loads on the soil may decrease rapidly and the excess~~remaining~~ high pore pressures, previously built up inside the soil during inundation, lead to upward directed forces within the soil matrix (Yeh and Mason 2014). ~~Excess pore pressure can be induced by external forces and is not released during tsunami draw-down for the case of soils with low permeability. Thereby, pore water pressures can accumulate up to the overburden weight pressure and reduce the vertical effective stress in the soil matrix (Yeh and Mason 2014). ASCE 7-16 Chapter 6 (2017) differentiates tsunami-induced pore pressure softening from seismic liquefaction. Whereas seismic liquefaction occurs during the high frequency shaking of the ground, pore pressure softening is the result of a long period inundation loading followed by a rapid drawdown, leading to an abrupt release of hydrostatic pressure.~~

Tonkin et al. (2003), Yeh et al. (2004) and Tonkin et al. (2013) derived an equation to describe the depth d_s of tsunami-induced liquefaction based on the one-dimensional consolidation model with an excess pore pressure field from Terzaghi (1925). These studies built upon a scour enhancement parameter, which defines the critical fraction of the buoyant weight of soil supported by pore pressure. Yeh et al. (2013) identified a tsunami-induced increase of pore pressure that reduced the shear strength of the soil around piles, leading to the structural failure of a four-story building in Onagawa. A recent numerical analysis of the pore water pressure in fully saturated beds under earthquake and tsunami-impact by Qiu and Mason (2019) stressed that hydraulic conductivity and soil layering strongly influence the pore water pressure response.

All in all, tsunami-induced soil instability is a potential threat to the overall stability of structures, as seen in a number of post-tsunami surveys e.g. in Dalrymple and Kriebel (2005), Yeh and Mason (2014) and Jayaratne et al. (2016).

2.3 Geotechnical Considerations

ASCE 7-16 Chapter 6 (2017) makes provisions for general erosion, local scour, and loss of shear strength as a result of pore pressure softening and displacement in the foundation design. General erosion has to be considered during run-up and draw-down. Special attention should be devoted to areas where flow velocity amplification due to the obstruction caused by buildings is possible, or at places where re-acceleration due to topography gradients and tsunami-induced pore pressure softening might occur (see Figure 2).

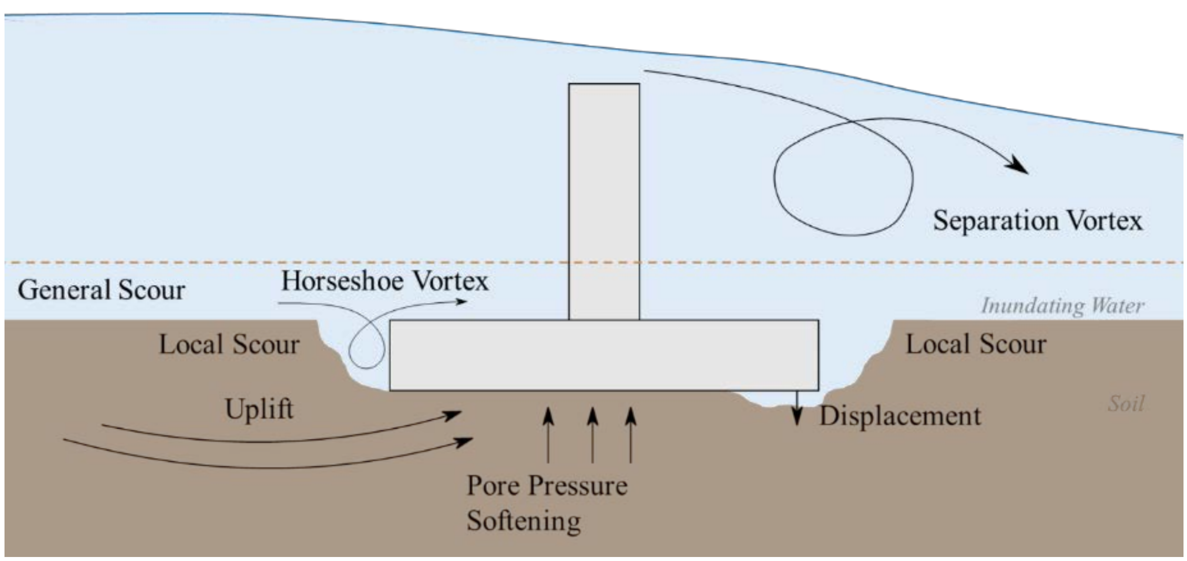

Figure 2: Soil considerations on a foundation system during tsunami inundation (adapted from ASCE 7-16, 2017).

ASCE 7-16 Chapter 6 (2017) considers sustained flow and plunging scour. ~~Sustained flow scour results from flow acceleration around structures and building corner piles, whereas plunging scour occurs where the tsunami flow passes over an obstruction~~

~~and drops onto the ground below (ASCE 7-16 2017).~~ Estimating ~~scour~~ depths of sustained flow scour can be accomplished by experimental and numerical modelling in cases where design equations are missing, or by employing stipulations given in ASCE 7-16 Chapter 6 (2017) ~~for sustained flow scour~~. This type of scour includes the effects of pore pressure softening due to rapidly changing water levels, which can be estimated with an empirical formula that depends on the flow depth. Flows with less critical flow velocities and lower abilities to initiate sediment transport are evaluated by means of the Froude number.

~~Plunging scour downstream of structures occurs when a flow overtops them.~~ Equations for estimating plunging scour depths are given in ASCE 7-16 Chapter 6 (2017) based on physical model results by Fahlbusch (1994), as described in Hoffmans and Verheij (1997), and the post-tsunami survey results of Tonkin et al. (2013), see Figure 3. Hydrodynamic and geometrical parameters are critical in these equations, though soil properties are not included.

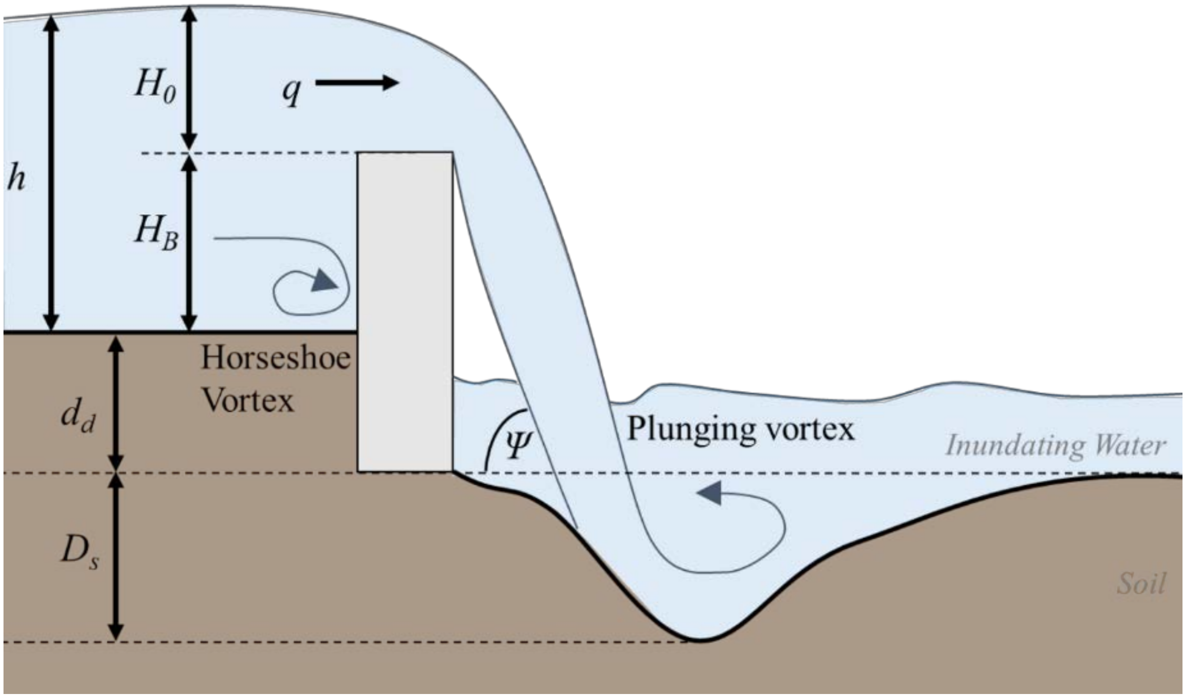

Figure 3: Parameters to describe the process of plunging scour (adapted from ASCE 7-16, 2017). These include the discharge (q), water depth (h), structure height (H_B), overtopping water depth (H_0), elevation difference (d_d), plunging scour depth (D_s) and the angle between the jet and the soil (Ψ).

Numerical and experimental modelling techniques can include the exposure of the structure and soil characteristics and thereby account for retention forces. Zhao et al. (2019) provided a numerical analysis of scour depths due to solitary and tsunami-like waves attacking different sea wall geometries. These authors concluded that the scour depth under tsunami-like conditions can be up to 4 times that under solitary wave conditions. McGovern et al. (2019) reported on an experimental investigation of scour depths around onshore structures induced by tsunami, and differentiate between maximum and final scour depth, as slumping was observed towards the end of inundation. Therefore, post-tsunami surveys might underestimate the maximum scour depth when measuring the final scour depth.

Even though latest research indicates dependencies between soil characteristics and scour depths, these parameters are not yet included in the geotechnical considerations of the

ASCE 7-16 (2017). Therefore, this post-tsunami survey aims at gathering field evidence to the interaction between tsunami and scour, taking into consideration local soil properties and hydrodynamic effects, in an attempt to facilitate dedicated future research.

3 Field Investigation

3.1 Site Locations

The field investigation covered the coastline starting from Loli Dondo on the west coast of Palu Bay to Wani on the east coast (see Figure 4), focusing on locations that were relevant for assessing damage due to hydrodynamic loading and associated sediment motion. Hydrodynamic loading is discussed at three locations, while new insights regarding general erosion were found at four ~~five~~ locations. The authors describe two locations with sustained flow scour and three cases that experienced channelized flow scour. Additionally, two locations where plunging scour was observed are also reported.

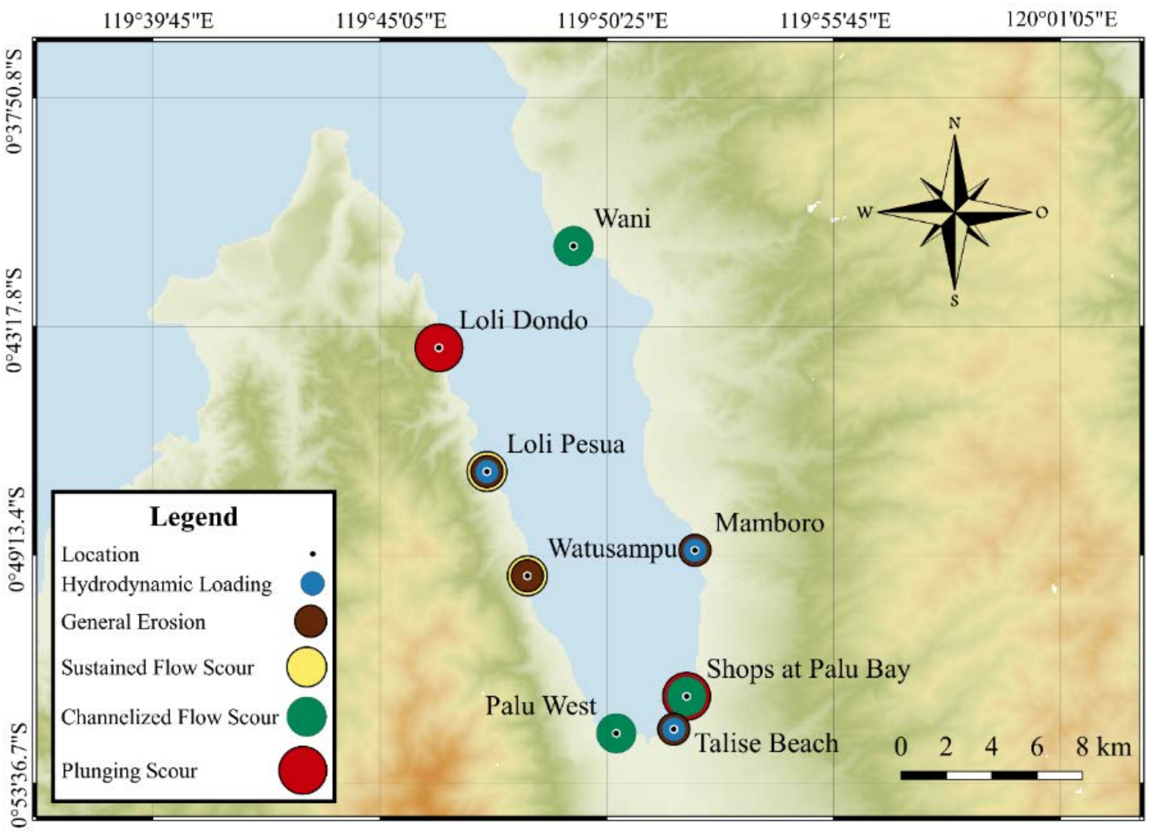

Figure 4: A selection of site locations visited during the field investigation.

Table 1 gives an overview of the survey locations, their geographical coordinates, local time of the site survey and concise descriptions concerning the observed effects.

Table 1: Descriptions of site locations mentioned throughout this study.

Number	Location	Longitude (degrees)	Latitude (degrees)	Local time when survey was conducted	Description
1	Loli Dondo	119.776	-0.731	28.10.2018 10:22	Local mosque damage by tsunami inundation and scour around satellite structures.
2	Loli Pesua	119.795	-0.780	28.10.2018 11:06	Small town with a house damaged by uplift of structural slab.
3	Watusampu	119.811	-0.821	28.10.2018 12:39	Military naval base with vessels washed onshore by tsunami.
4	Palu City	119.846	-0.884	28.10.2018 16:23	Local scour around a foundation pile along a former wall.
5	Talise Beach - Palu Pavilion	119.869	-0.882	29.10.2018 10:43	Lookout over Palu Bay, damaged by uplift forces.

6	Shops at Palu Bay	119.872	-0.869	29.10.2018 12:17	Destroyed shops at Palu Bay with sustained flow scour, plunging scour and general erosion.
7	Mamboro	119.877	-0.811	29.10.2018 12:50	Fuel tanks damaged by uplift forces as result of large displaced water volumes.
8	Wani	119.829	-0.690	29.10.2018 17:30	Large cement plant damaged by earthquake, significant scour around the foundation.

3.2 Tsunami Characteristics

The 2018 Palu Tsunami consists of a complex interaction of waves generated by seismic action and concurrent landslide dynamics. An analysis by Sassa and Takagawa (2018) implied that less than 20 % of the tsunami height was generated by tectonic processes directly related to the earthquake, with submarine landslide generated waves inducing the remaining. Further amplification of the wave height took place due to the energy focussing effects of Palu Bay towards Palu City, with tsunami waves of various origins superimposing in a wave-amplifying fashion (Aránguiz et al. 2019).

Field surveys indicate run-up heights ranging from 0.3 m to 8.0-9.0 m along the circumference of Palu Bay (Omira et al. 2019, Carvajal et al. 2019, Mikami et al. 2019). The inundation depths for site-specific locations outlined in the following section were measured using a laser-ranging instrument (Impulse 200LR, Laser Technology Inc., +/- 0.01 m). Generally speaking, lower run-up heights were found on the north west side of Palu Bay near the town of Donggala, while higher run-up heights were mostly observed in the south of the bay. Run-ups heights of 8.0 m were recorded along Watusampu (Carvajal et al. 2019), 6.0-7.0 m in Talise (Omira et al. 2019), 1.5-4.5 m in Palu (Mikami et al. 2019, Widiyanto et al. 2019) and 4.0-5.0 m at Wani (Omira et al. 2019, Carvajal et al. 2019).

Inundation distances varied depending on the local topography and wave characteristics. Putra et al. (2019) and Widiyanto et al. (2019) concluded that the inundation distance ranged from 65~~.36~~ m at areas with steep slopes such as Loli Dondo to nearly 500 m in the north of Talise Beach (which had a flat topography). In Palu City the tsunami travelled approximately 250 m inland due to the flat dense urban geography (Mikami et al. 2019, Widiyanto et al. 2019).

Eyewitnesses interviewed by the authors reported that the first wave of the tsunami arrived at different locations between 3 to 10 minutes after the earthquake, and that a total of three waves affected the shoreline of Palu Bay.

All in all, there is a wide variation of run-up heights and inundation distances along Palu Bay, though all are characterised by their relative high wave height and short periods. Therefore, the damage to structures at each location should be assessed based on locally surveyed wave heights and inundation depths.

3.3 Characteristics of Structures and Sediment

Residential buildings in the Palu area have a variety of construction designs, with Figure 5 showing typical light timber constructions, some of which had concrete frames filled with masonry walls or metal sheets (Figure 5 b). Some buildings were constructed out of reinforced concrete, and exhibited greater stability. Many timber constructions and masonry infill walls failed due to tsunami loading (Figure 5 a-c) while solid concrete frames were mostly able to withstand the tsunami impact.

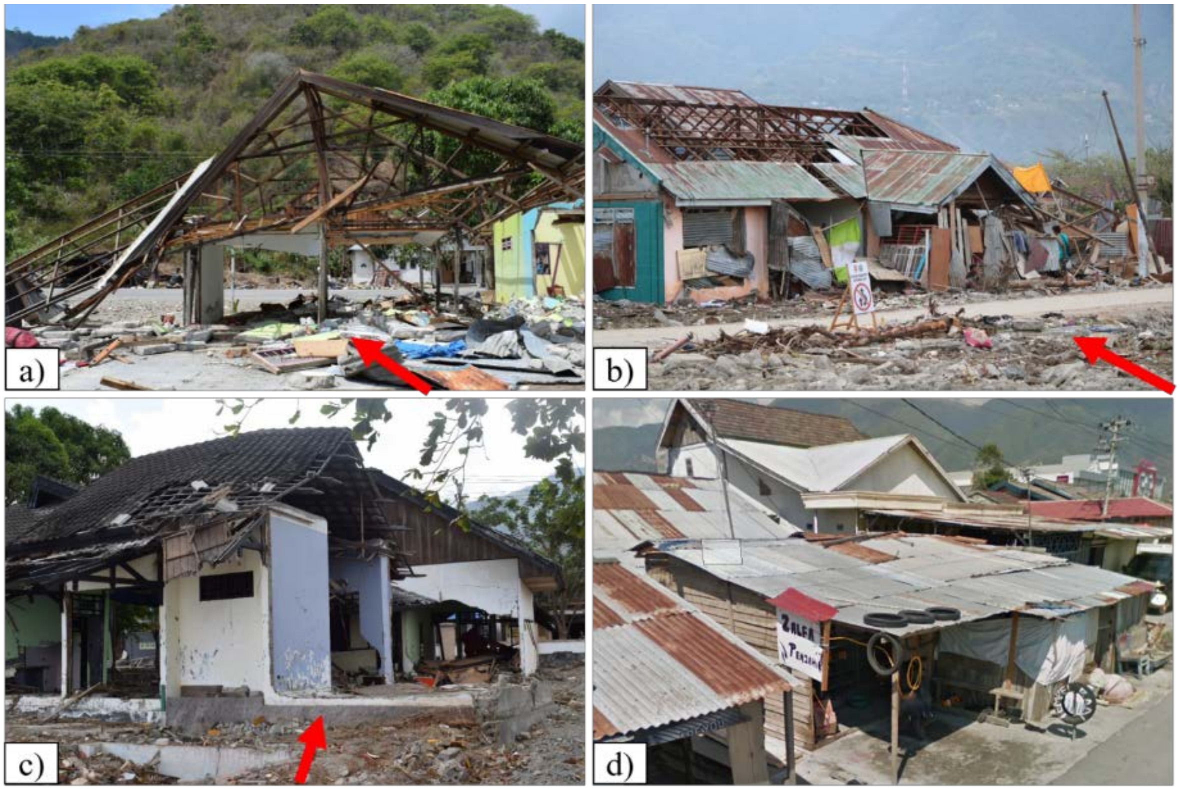

Figure 5: Typical buildings in Palu City with red arrows indicating the approximate direction of the incoming wave. Pictures a-c) show damaged or demolished buildings, as observed during the post-tsunami survey, while d) is a picture obtained from Google Earth of a simple timber structure in Palu City which was washed away.

Soil material varied around Palu Bay depending on the location along the coastline and the distance to the shoreline. Figure 6 a) was taken in Palu west and shows fine sediment grains with a rather uniform diameter, while locations near a Palu City shopfront (b), Palu east (c) and Wani (d) show a wide-graded grain size distribution. Generally, the sediment material seemed to be fluvial material with round grains, rather than crushed material with sharp edges. A visual inspection of variation in grain size diameters could help explain some of the exposure and hiding effects discussed later in this paper. However, no soil samples could be taken in this survey, which would allow for performing a sieve curve analysis and investigating soil effects more quantitatively.

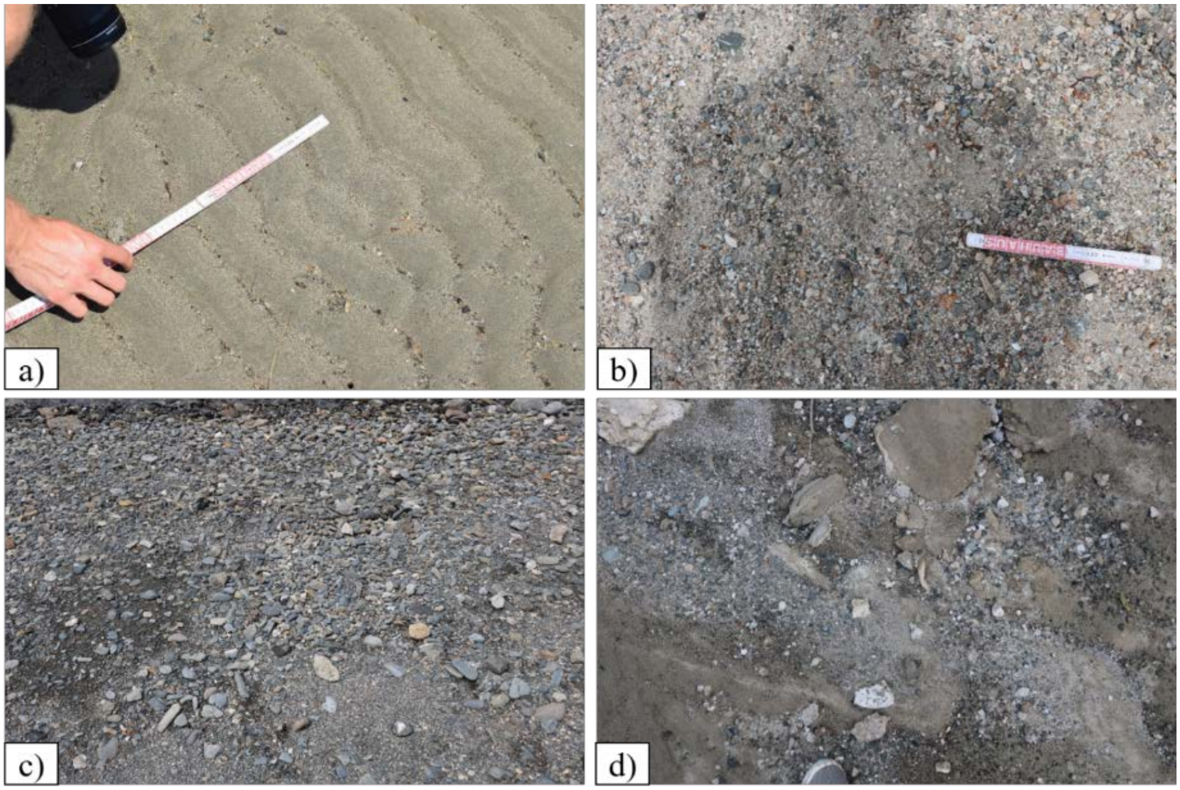

Figure 6: Sediment types observed in Palu, Indonesia. a) A ruler was placed to obtain a rough estimate of the average grain diameter for Palu west, b) at a shopfront in the east of Palu, c) north of Talise Beach and d) in Wani.

4 Observed Effects of Tsunami Inundation

4.1 Uplift Forces

Hydrodynamic loading is typically attributed to the tsunami flow interacting with structures, either around or beneath them (drag and lift). A highly turbulent tsunami bore travelling inland of a coastal area can be characterized by highly fluctuating flow depths and velocities (Chanson 2009). These characteristics of hydrodynamic forces can induce both uplift and horizontal forces ~~components~~ on structures (Palermo et al. 2013). The effects of vertical uplift forces during tsunami inundation were observed~~found~~ during the survey at many locations, including Loli Pesua, the Pavilion at Talise Beach and Mamboro (see Figure 4).

Loli Pesua is a small town located 15 km north-west of Palu City. A road situated 2-3 m above sea level traverses the town at a distance of 20 to 50 m from the coastline. The tsunami run-up height at this location was measured to be 3.9 m (Omira et al. 2019). A site-cast concrete building located on the leeside of the road was affected by the tsunami, see Figure 7. A retaining wall and two rows of concrete columns, each with four columns (0.3 m × 0.3 m × 2.1 m) parallel to the shoreline, supported the building. Reinforced concrete was used for the frame elements whereas the walls and slab consisted of masonry infill. The frame elements withstood the tsunami impact, though vertical uplift forces on the bottom slab were induced by the incoming tsunami, as its progress was impeded by the retaining wall.

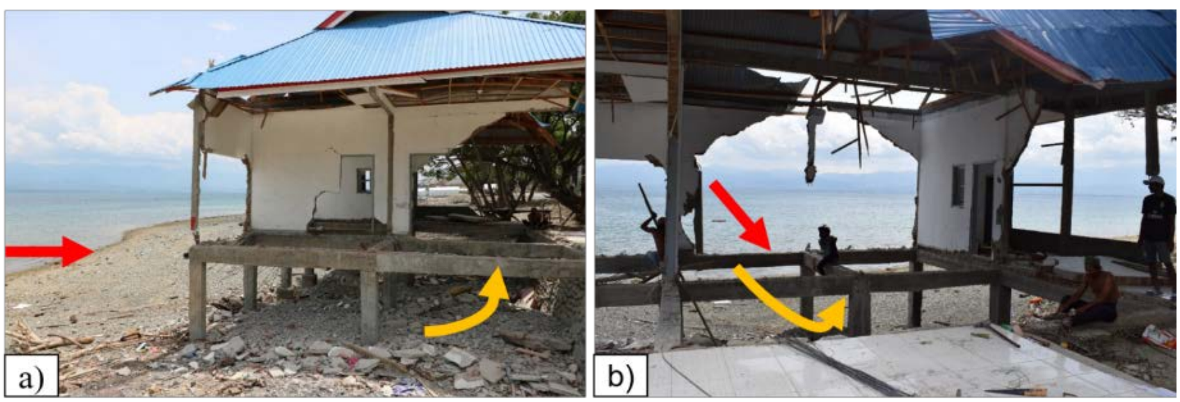

Figure 7: Site-cast concrete building in Loli Pesua. a) View of the building from the beach and b) showing the destruction to the slab. Red arrows indicate the incoming tsunami flow direction, while yellow arrows indicate the likely flow path under the building.

Figure 8 shows the Pavilion at Talise Beach on the east side of Palu City, which serves as a lookout over the bay and is located directly on the coastline, roughly 1 m above sea level. Twelve foundation piles and a retaining wall support the slab. Radial joists directed towards the centre of the semicircle-formed slab connected the piles. Ruptures along the concrete columns indicate that vertical uplift forces were induced due to the tsunami flow entrapped in the wall-slab recess, a situation very similar to what was observed at Loli Pesua.

Figure 8: The Pavilion located on the east side of Palu City overlooking Palu Bay in a-b). c) Vertical uplift damage was observed through cracks in the piles and in the rear anchoring and d) in the aesthetic tiling. Areas of interest are highlighted by arrows and dotted lines to indicate uplifted tiles and erosion.

Damage to both structures seems to have been enhanced by the construction methodology, with a bottom slab placed above joists in front of a retaining wall. This phenomenon of tsunami flow entrapped in structural wall-slab recesses is considered by ASCE 7-16 Chapter 6 (2017) for incoming bore conditions, but no guidance is provided for non-bore (surge) conditions due to the lack of experimental data (Ge and Robertson 2010). Given that the obstructed flow may have developed during the initial approach of the tsunami, it is very likely that a pressure imbalance between hydrostatic and hydrodynamic components led to forces acting in the vertical direction. The uplift force could have moved the slab slightly upwards, as ruptures were found along the concrete columns and at the anchoring to the retaining wall. ASCE 7-16 Chapter 6 (2017) requires that slabs associated with these slab-wall recesses be designed for an uplift pressure of 16.76 kPa (350 psf), which would explain the damage observed in these two survey cases.

Inland from the lookout, a two-part sidewalk was found consisting of concrete slabs (Figure 8 a, d). The first row (located behind the lookout step) was heavily damaged and had been transported away, while the second row remained almost unaffected. Water pressure passing the elevated slab may have contributed to uplift of the sidewalk as well as negative pressures due to surpassing flow over the elevated slab. A comparable geometry to investigate separation and reattachment of surpassing flows is the backward-facing step, which has been extensively analysed. This case is often used as a reference for numerical simulations to evaluate the representation of flow phenomena using a simple geometry (Eaton and Johnston 1981, Le et al. 1997, Ratha and Sarkar 2015, Chovet et al. 2018, Wang et al. 2019). Adams and Johnston (1988a, 1988b) found the flow between the wall and the reattachment point to be directed towards the wall, leading to the formation of a vortex and positive pressure gradients. Chovet et al. (2018) analysed pressure distributions and the flow structure, emphasizing the formation of negative pressures upstream of the reattachment point and a forcing roll-up of the vortices. In the Palu lookout, the negative pressures due to the formation of a vortex led to uplift forces in the pavement, which may have caused the destruction of the first row. Comparable mechanisms led to dike failures during the 2011 Tohoku Earthquake and Tsunami, where Kato et al. (2012) found that high flow velocities induced negative pressures at the top of dikes, which lifted up landward and crown armor and led to the failure of the structure.

Buoyancy and vertical uplift forces were observed in this field survey at multiple locations, leading to the failure of many structures, particularly when both of these acted simultaneously (with this load combination probably causing the failures shown in Figure 7 and 8). The uplift forces caused by a tsunami bore flow that is blocked by solid walls are considered in ASCE 7-16 Chapter 6 (2017), as mentioned earlier. The uplift pressure depends on the ratio of slab soffit elevation to flow depth. Robertson (2014) compared small and large scale experiments concerning uplift forces on slabs with a solid wall blocking the tsunami bore flow behind the slab, showing that maximum uplift pressures of up to 1.4 times the maximum design pressure for ratios of slab soffit elevation to flow depth of 1.0 to 1.5. This maximum might be related to pressure shocks by entrapped air, which is not considered explicitly in ASCE 7-16 Chapter 6 (2017). The investigation of load combinations leading to uplift as a consequence of highly turbulent tsunami flows acting on slabs (including entrapped air as well as blockage by retaining walls) is a significant failure mechanism observed during this field survey.

More recently, studies such as Seiffert et al. (2015), Moideen et al. (2019) and Seiffert et al. (2014) have started to look into total vertical forces of solitary and cnoidal waves on coastal bridge decks with openings where entrapped air has the potential to add to the overall force balance by increasing buoyancy. For future studies, it would be crucial to investigate the destabilizing effect of entrapped air within structures exposed to extreme flow conditions, such as broken solitary waves or bores.

4.2 Soil Instability

4.2.1 General Erosion

Throughout the post-disaster survey, erosional patterns and soil instabilities were frequently observed, leading to widespread erosion. Loss of soil support around foundations was found at structures located close to the shoreline, jeopardizing their overall stability. The high flow velocities of the tsunami increased the shear forces on the sediment, leading to suspension transport of the particles. Although a quantification of the amount of sediment or the erosion depths was difficult, as the elevation of the land prior to the tsunami event was not known, some ~~areas~~ interesting areas are outlined below (see Figure 9).

Figure 9: Eroded areas were found on a) the west coast in Loli Pesua, b) in Watusampu. On the east side of Palu Bay general erosion was observed in c) near the landslide north of Talise and d) at the Mamboro fuel station. Red arrows indicate the flow direction of the incoming tsunami, red dotted lines show the erosion extent while yellow dotted lines show the approximate slope indicating discontinuities.

General erosion was found to be accompanied by local discontinuities in the soil matrix, which was observed both on the west coast (see Figure 9 a, b) and on the east coast (Figure 9 c, d) of Palu Bay. Strong discontinuities in the soil matrix were observed at widely-graded soil compositions both in Loli Pesua (Figure 9 a) and at the Mamboro fuel station (Figure 9 d). Narrowly-graded soil compositions were found in front of the discontinuities with larger depths of general erosion. ~~While the erosion at the west coast~~

could be identified by discontinuities in the soil matrix (see Figure 9 a, b), the east side exhibited more uniform soil erosion (Figure 9 c) or an edge in the soil as a result of varying soil stability (Figure 9 d). A lack of consistency in soil composition can enhance influences general erosion, particularly when infilling soil material is present. Designing tsunami-safe foundations requires reliable assessment of soil stability and soil effects during tsunami inundation, which highlights the importance of an accurate analysis of soil properties in order not to weaken the soil matrix (as discussed earlier, see also Schendel et al. (2016), Schendel et al. (2018) and Shvidchenko et al. (2001) for a description of the soil stability of wide-graded material in extreme flow conditions).

4.2.2 Sustained Flow Scour

Four reinforced concrete columns in a building near Watusampu Naval Base were damaged as a result of sustained flow scour around their foundations, as seen in Figure 10 a-c). All four columns were supporting a balcony, and were 0.5 m in length and 0.35 m in width. Gravel material supporting the column foundations was eroded, resulting in a final scour depth of approximately 1.1 m. A naval vessel was transported with the flow to higher ground, indicating inundation heights of more than 3 m. According to Andiani et al. (2018), the inundation depth was approximately 4.8 m at the Naval Base. Referring to Chapter 6 of ASCE 7-16 (2017), a maximum scour depth of 3.66 m is reached when the inundation depth exceeds 3.05 m. The scour at this site is well within this ASCE 7-16 Chapter 6 (2017) design limit.

Figure 10: Effects of sustained flow scour around columns (a-c) in Watusampu and d) around the edge of a bottom slab in Loli Pesua. Red arrows indicate the approximate wave direction and yellow arrows show the likely flow path.

Severe damage occurred at two columns on the south east side of this building, where the lack of supporting material led to a decrease in structural stability (Figure 10 c). Tsunami-induced scour adjacent to the column foundations resulted in a decrease in the soil loadbearing capacity. As the scour was larger on the south side, the foundations of both columns moved 0.7 m to the south, resulting in a column inclination angle of approximately 10°. The dislodged foundation led to heavy damage at the interface between the columns and the supported beams, with only exposed reinforcement bars maintaining any connection. This is an indication of tension failure, probably due to subsidence of the foundation elements. Based on several cracks found in the joists and columns, the overall stability of the balcony and the seaward side of the building has been significantly affected by the sustained flow scouring.

Further scouring was observed behind the second row of columns in the building structural frame (Figure 10 b). Scour around the columns enabled the flow to further remove sediment under the bottom slab of the building. This bottom slab was made of concrete and masonry infill, and was presumably not designed to resist its own self-weight, so it suffered heavy damage when the supporting soil was removed.

Another area with indications of sustained flow scour is Loli Pesua, with Figure 10 d) showing its effects on a concrete slab situated along the coastline. The load-bearing capacity of the concrete slab was still present, but it can be assumed that the loss of soil under it due to the tsunami flow reduced structural stability. The scour depth was up to 0.5 m at the edge of the concrete slab and extended approximately 0.3 m under the slab. The supporting soil material was widely graded and had median grain size diameters of silt between 0.0063 mm - 0.02 mm.

According to ASCE 7-16 Chapter 6 (2017), sustained flow scour can be estimated using empirical guidelines available in literature or, for cases with pore pressure softening, with the aid of physical or numerical models. Tonkin et al. (2013) and Tonkin et al. (2003) developed analytical solutions to calculate the scour depth depending on the water depth, though they do not include the velocity-induced bottom shear stress, typically used to describe the initiation of sediment motion (Sumer and Fredsoe 2002). Further uncertainty may stem from the characterization of the soil by a single grain size without including the grain size distribution, ~~and~~ associated hiding and exposure effects~~, or the of the soil~~ and the ~~associated~~ entrapped air (Tonkin et al. 2013). In accordance with the observations made in Watusampu, current design methods seem to contain large safety margins due to a lack of knowledge about the influences of soil properties on sustained flow scour.

4.2.3 Channelized Flow Scour

Constrictions between rigid structures force the flow to accelerate because of reduced cross-sectional area. This leads to flow velocity increases, which result in increased shear stresses acting on the soil. This phenomenon can be described as scouring induced by channelized flow, which can cause high scour depths (though in general the extent is small, as it is caused by high volume fluxes affecting small cross sections, see ASCE 7-16 (2017). The site locations showing channelized flow scour investigated during this survey are shown in Figure 11.

Figure 11: Local and channelized flow scour a) on the northern and b) southern corner of the Shops at Palu Bay. c) Scour besides a column foundation. The sheet metal wall on the right side replaces a masonry wall which was destroyed during the tsunami. d) Scour around the silos of a cement packing plant north of Wani. Red arrows indicate the incoming tsunami wave direction while the red dotted lines show the scour extent.

Local scour in channelized flow conditions was observed on the north-west and on the south-east side of the shops at Palu Bay. On the north-west, local scour around a building corner was observed. A wall built on the seaward side led to high flow velocities beside it (Figure 11 a), the wall is highlighted in blue ~~black~~). The maximum scour depth of 1.04 m was found directly at the building edge, where the horizontal extent of the scour hole was 3.14 m in the seaward direction and 2.5 m parallel to the coastline. Similar processes can be seen next to the south-east corner, where an irrigation channel forced the flow between the structure and the wall (Figure 11 b). In this constriction the flow induced high shear stresses and thus an increased amount of scouring. The scour depth near the foundation measured up to 1.3 m.

On the western side of a building next to the Institut Agama Islam Negeri (IAIN), a sheet metal wall was constructed after the tsunami had damaged an earlier masonry wall (which was washed away, along with paving stones in front of the building, see Figure 11 c). In front of the foundation pile, the pavement was lifted and the underlying sediment was eroded. The channelizing by the masonry wall (right side in Figure 11 c) resulted in scour with a horizontal extent of 4.3 m in the seaward direction and 2.0 m along the building edge. The maximum scouring occurred right in front of the foundation pile, with a depth of 1.2 m.

At a cement packing facility about 30 km north east of Palu City concrete slabs surrounding two silos were affected by scouring on the landward (Figure 11 d) and seaward sides. The distance to the coastline prior to the tsunami was about 10 m. The scour between the two silos on the landward side had a lateral extent of 2.8 m and a maximum depth of 1.1 m. As seen from the coastline, scour was also observed in front of the left silo, with a lateral extent of 1.5 m and a maximum depth of 1.3 m. Eyewitnesses reported that the initial separation of the connecting slab and tilting of one of the silos was caused by the earthquake, while the subsequent tsunami scoured the soil below and around the slab, further destabilising it.

ASCE 7-16 Chapter 6 (2017) references Nouri et al. (2010) who provide empirical equations based on physical experiments concerning current amplification in obstructed flows. These experiments were conducted for a limited amount of blockage ratios (ratio of obstruction width to flume width). Small scale channelization, as seen in Figure 11, with blockage ratios below 0.125 and with inclined flow paths, was not investigated. To prevent structural failure due to channelized scour, extensive studies of flow path geometries and blockage ratios could help to provide more accurate design guidelines.

4.2.4 Plunging Scour

In Loli Dondo, a wall was built a few meters from the shoreline on the south side of the mosque Masjid Ar-Rahman Loli Dondo (Figure 12 a). During the tsunami, the wall was overtopped and the flow impinged on the soil behind, which caused plunging scour. Besides the plunging scour effect, the tsunami draw-down might have also caused some of this scour (when gravitational forces due to the scour hole accelerated the flow, which could have resulted in a roller-like wave motion further eroding the inland side of the wall). The scour occurred along the entire wall at this location, with a depth of about 0.5 m and a length in the landward direction of about two to five meters.

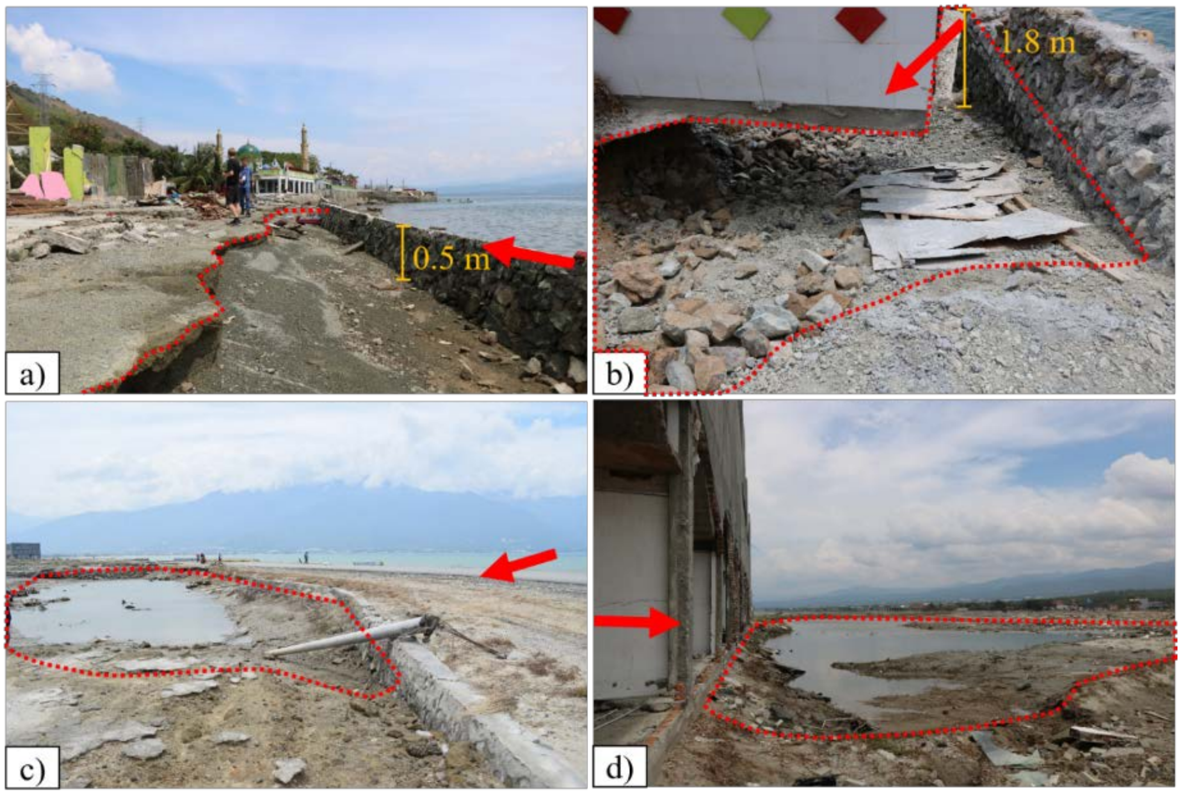

Figure 12: Plunging scour behind walls in Loli Dondo a) in the south and b) in the north. c) Plunging scour behind a retaining wall near a construction site and d) behind the shops at Palu Bay. The approximate scour extent is shown in red while the red arrows indicate the wave direction.

North of the mosque in Loli Dondo, a circular wall was overtopped by the tsunami, and plunging scour led to sediment loss between the wall and a platform (Figure 12 b). The scour depth behind the wall was around 1.8 m resulting in the partial failure of the wall and in a large amount of eroded sediment, which was meant to support the platform. The sediment was wide-graded and mostly broken pebbles ~~gravel~~ (d_{50} = 1-4 cm). Similar processes to those described earlier might have been involved in this site, with the initial wave plunging to the backside of the wall, scouring the area behind it and leading to the saturation of the soil beneath. Finally, the receding wave could have taken the saturated sediment water mixture with it, with a roller-like wave motion enhancing sediment transport.

Around the shops at Palu Bay in panel c) and d) of Figure 12, general erosion, sustained flows and plunging scour could be observed. These shops were situated at distance of 30 m from the coastline, at an elevation of 4 m above sea level. After the incoming tsunami propagated through the shops in Figure 12 d), the water plunged down and scoured the soil behind the shops. No information about the terrain elevation prior to the tsunami could be found.

About 500 m north of the shops a retaining wall between the road and a construction site was overtopped by the flow, see Figure 12 c). The spatial extent of the scour was comparable to an ellipse with a long side of about 40 m (parallel to the coastline) and the short side (orthogonal to the coastline) of about 10 m in length.

Plunging scour in Loli Dondo indicates the possibility of self-reinforcing soil effects that can enhance scour during tsunami inundation. Initial plunging forms a scour hole, which might be enhanced by sustained flow scour. When the water stays inside the scour hole, the pore pressure adjusts to the hydrostatic pressure. Further sediment transport is initiated if momentary liquefaction occurs during the receding wave, due to the sharp decline in hydrostatic pressure. Structural stability could be greatly affected due to the creation of large scour holes beside the foundations.

4.3 Scour-induced Structural Failure

On the east side of Palu Bay, approximately 5 km north of Palu City, the survey team surveyed a construction site located 30 m from the shoreline (Figure 13 a). Scour under the slab-on-grade was observed at various locations in the building, as high velocity flows passed over the structure and plunged down. This could have induced negative pressures on the slab-on-grade and in the soil due to the presence of joints between the slab and edge beam, which induced uplift and led to the failure (refer to Figure 2).

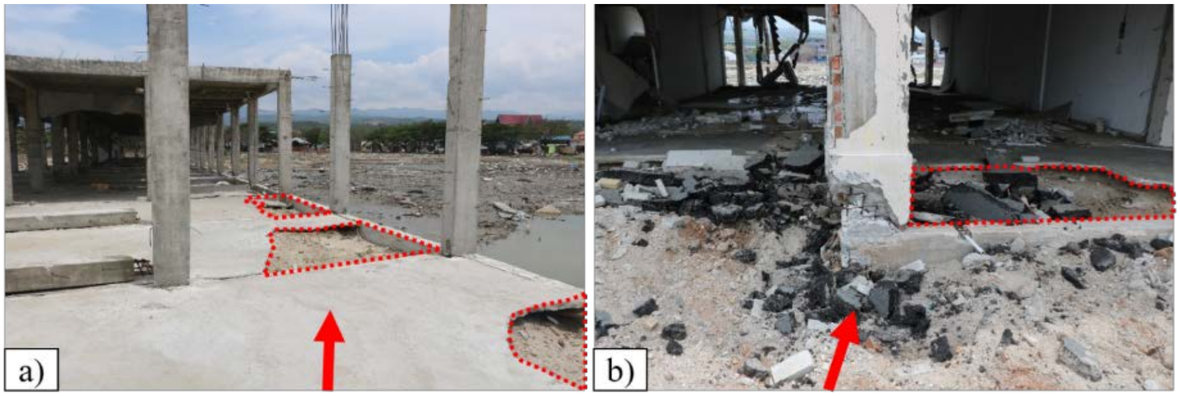

Figure 13: a) Scour under the slab of a construction site on the east side of the bay in and b) scour in front of a column and under the slab of the shops at Palu Bay. Red dotted lines indicate the areas of interest while the red arrow shows the approximate wave direction.

Scour underneath foundations was observed at the shops at Palu Bay (Figure 13 b). Similar to the case of the construction site, the sediment underneath the slab could have been pressurized by the flow separation after passing the slab edge beam. Figure 14 shows a sequence of the possible process of the damage that could have lead to the failure of the slab in Figure 13 b). Debris was found inside the building, which may have damaged the tiles upon impact and thereby lead to a partially damaged slab. These debris were probably asphalt pieces released from the street adjacent to the construction site and transported with the flow. The water flow intruded into these partially damaged slabs, allowing for pressurization or erosion of the supporting sediment, and led to further scouring. The spatial extent of damage to the bottom slab ~~destruction~~ varied depending on the local hydrodynamic conditions, which may be overlapped with initial damage caused by debris as entry points for scouring.

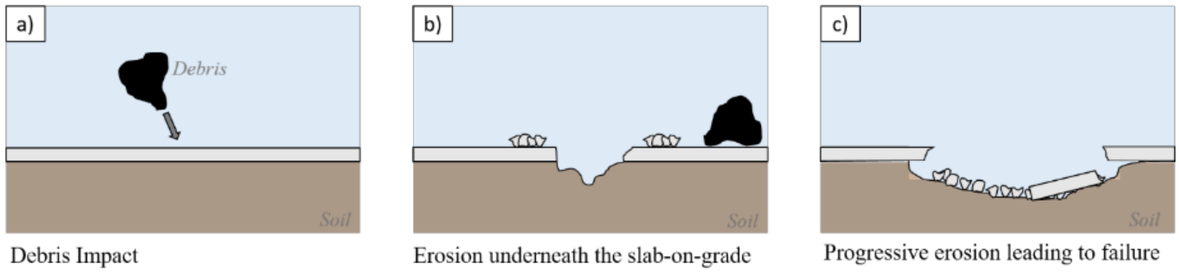

Figure 14: Combined loading of tumbling debris impact, sediment erosion and subsequent failure.

5 Engineering Lessons Learned

Based on the observations outlined earlier, a range of structural engineering lessons and conclusions could be obtained, some of which are only partially addressed in current tsunami guidelines:

(1) ASCE 7-16 Chapter 6 (2017) considers uplift forces on wall-slab recesses for bore conditions based on the experimental results of Ge and Robertson (2010) and Takakura and Robertson (2010). However, this research has primarily focused on bore flow conditions, whereas surge conditions have not yet been included in tsunami design guidelines.

(2) Pressure distributions and sediment transport due to the formation of vortices or roller-like wave motions were seen to be important mechanisms behind solid structures. Hydrodynamic loading associated with separation and reattachment flow over backward-facing steps, as well as soil instabilities due to the formation of roller-like wave motions, induced negative pressures and led to failure at the Pavilion at Talise beach and enhanced sediment transport at Loli Dondo. Further systematic research of reattachment lengths and pressure distributions associated with the roll-up of vortices is necessary in order to provide guidelines for coastal

structures such as dikes and breakwaters, where negative pressures might lead to enhanced sediment transport or even structural failures.

(3) Maximum scour depths are defined in ASCE 7-16 Chapter 6 (2017) and are based on post-tsunami field observations and take into account the design inundation depth, whereas the most crucial parameter for sediment transport is the applied shear stress, which depends mainly on the flow velocity. Despite the fact that the flow velocity and inundation depth are linked, several uncertainties in describing the tsunami-bore velocity and direction exist when estimating flow velocities of a bore travelling over land (Nistor et al. 2009). These uncertainties are relevant for assessing structural damages as well as the effect of the flow on the soil, which makes it crucial to gain further insights into the tsunami inundation velocity under bore and non-bore conditions.

(4) Grain sizes and gradation vary greatly along the coastline of Palu Bay. The influence of hiding and exposure effects on the soil stability have only recently started to be addressed, and are not taken into account in existing tsunami engineering guidelines. More research must be performed on flows with long wave periods, such as tsunamis, and their influence on wide-graded sediment material. Additionally, the influence of wide gradation is not included in tsunami design procedures concerning pore pressure softening and related liquefaction, which is an additional research area to focus on.

(5) A large extent of plunging scour of wide-graded soil material was observed in Loli Dondo and near the shops at Palu Bay. To improve the erosion stability of soils near foundations, the influence of gradation on time-dependent pore water pressures in plunging scour environments should be investigated.

(6) Pore pressure softening is a crucial soil effect during tsunami inundation, which can affect general erosion as well as scour. The quantitative impact of pore pressure softening on soil erosion cannot be determined during post-tsunami field surveys due to limitations in data acquisition. Therefore, further systematic research is needed to determine and understand the governing hydrodynamic and geotechnical parameters. Physical system understanding could be improved for example by employing model tests in large-scale facilities with the overarching goal to establish process-based design equations.

(7) Load combinations can cause more severe damages than single load cases. Initial debris impact on slabs can facilitate scouring underneath it, leading to its destruction, as was seen in newly constructed buildings on the east side of Palu. This was established for a single load case, though further load case combinations should be determined and investigated to be able to predict subsequent failures.

6 Conclusions

Post-tsunami survey findings in the aftermath of the 2018 Palu tsunami were presented and compared with tsunami design guidelines (ASCE 7-16 2017) and the latest research in the field of hydrodynamic uplift forces and geotechnical considerations, such as erosion, scour and pore pressure softening. The structural failures of slabs due to negative pressures were seen to occur due to local varying flow velocities. While giving straightforward tsunami design guidelines, Chapter 6 in ASCE 7-16 (2017) relies mostly on simplified empirical guidelines, which can be complemented by newer research findings. Further research regarding uplift forces on wall-slab recesses during surge conditions could reduce the costs of building tsunami resilient communities where bore conditions do not apply. Another key finding is the dependency between soil effects and the gradation of sediment grains. The influence of hiding and exposure effects on wide-graded sediment should be further investigated in order to provide reliable dynamic assessments of scour depths during tsunami inundation. To conclude, the findings of this and other surveys provide the opportunity to direct research activities and the development of engineering methods to aid in the design of tsunami-resilient communities.

Data Availability Statement

All data, photographs, or sketches that support the findings of this study are available from the corresponding author upon reasonable request.

Disclosure Statement

No potential conflict of interest was reported by the authors.

Acknowledgements

A part of the present work was performed as a part of activities of Research Institute of Sustainable Future Society, Waseda Research Institute for Science and Engineering, Waseda University, Tokyo, Japan.

References

Adams, E. W., and J. P. Johnston. 1988a. Effects of the separating shear layer on the reattachment flow structure - Part 2: Reattachment length and wall shear stress. Experiments in Fluids 6:493–499. doi: 10.1007/BF00196511.

Adams, E. W., and J. P. Johnston. 1988b. Effects of the separating shear layer on the reattachment flow structure - Part 1: Pressure and turbulence quantities. Experiments in Fluids 6:400–408. doi: 10.1007/BF00196485.

Andiani, O. Oktariadi, and A. Kurnia. 2018. Di Balik Pesona Palu: Anomali Perilaku Gelombang Tsunami. . Badan Geologi.

Aránguiz, R., M. Esteban, H. Takagi, T. Mikami, T. Takabatake, M. Gómez, J. González, T. Shibayama, R. Okuwaki, Y. Yagi, K. Shimizu, H. Achiari, J. Stolle, I. Robertson, K. Ohira, R. Nakamura, Y. Nishida, C. Krautwald, N. Goseberg, and I. Nistor. 2020. The 2018 Palu Tsunami as a combination of several landslides and co-seismic tsunami effects. Nature.

Arikawa, T., A. Muhari, Y. Okumura, Y. Dohi, B. Afriyanto, K. A. Sujatmiko, F. Imamura, and, and, and, and, and and. 2018. Coastal Subsidence Induced Several Tsunamis During the 2018 Sulawesi Earthquake. Journal of Disaster Research 13:sc20181204. doi: 10.20965/jdr.2018.sc20181204.

ASCE 7-16. 2017. Minimum Design Loads and Associated Criteria for Buildings and Other Structures. . American Society of Civil Engineers.
Bahar, I., I. Effendi, E. T. Putranto, and D. Sukarna. 1997. Earthquake Monitoring in Indonesia. . Islamic Educational, Scientific and Cultural Organization (ISESCO).
Bihs, H., A. Kamath, M. A. Chella, A. Aggarwal, and Ø. A. Arntsen. 2016. A new level set numerical wave tank with improved density interpolation for complex wave hydrodynamics. Computers & Fluids 140:191–208. doi: 10.1016/j.compfluid.2016.09.012.
Bricker, J., M. Francis, and A. Nakayama. 2012. Scour depths near coastal structures due to the 2011 Tohoku Tsunami. Journal of Hydraulic Research 50:637–641. doi: 10.1080/00221686.2012.721015.
Carvajal, M., C. Araya-Cornejo, I. Sepúlveda, D. Melnick, and J. S. Haase. 2019. Nearly Instantaneous Tsunamis Following the Mw 7.5 2018 Palu Earthquake. Geophysical Research Letters 46:5117–5126. doi: 10.1029/2019gl082578.
Chanson, H. 2009. Current knowledge in hydraulic jumps and related phenomena. A survey of experimental results. European Journal of Mechanics-B/Fluids 28:191–210.
Chovet, C., M. Lippert, L. Keirsbulck, and J.-M. Foucaut. 2018. Unsteady Behavior of a Backward-facing Step in Forced Flow. Flow, Turbulence and Combustion 102:145–165. doi: 10.1007/s10494-018-9944-0.
Dalrymple, R., and D. Kriebel. 2005. Lessons in engineering from the tsunami in Thailand. The Bridge 35:4–13.
Eaton, J. K., and J. P. Johnston. 1981. A Review of Research on Subsonic Turbulent Flow Reattachment. AIAA Journal 19:1093–1100. doi: 10.2514/3.60048.
Fahlbusch, F. E. 1994. Scour in rock riverbeds downstream of large dams. The International Journal of Hydropower & Dams.
Francis, M. J. 2006. Tsunami Inundation Scour of Roadways, Bridges and Foundations - Observations and Technical Guidance from the Great Sumatra Andaman Tsunami. . EERI/FEMA NEHRP Professional Fellowship Report.
Fraser, S., A. Raby, A. Pomonis, K. Goda, S. C. Chian, J. Macabuag, M. Offord, K. Saito, and P. Sammonds. 2013. Tsunami damage to coastal defences and buildings in the March 11th 2011 Mw9.0 Great East Japan earthquake and tsunami. Bulletin of Earthquake Engineering 11:205–239. doi: 10.1007/s10518-012-9348-9.
Ge, M., and I. N. Robertson. 2010. Uplift Loading on Elevated Floor Slab due to a Tsunami Bore. . University of Hawaii, Manoa.
Goseberg, N. 2013. Reduction of maximum tsunami run-up due to the interaction with beachfront development–application of single sinusoidal waves. Natural Hazards and Earth System Science 13 (2013), Nr. 11.
Hoffmans, G. C. J. M., and H. J. Verheij. 1997. Scour Manual. . A. A. Balkema.
Jayaratne, R., B. Premaratne, A. Abimbola, T. Mikami, S. Matsuba, T. SHIBAYAMA, M. Esteban, and I. Nistor. 2016. Failure Mechanisms and Local Scour at Coastal Structures Induced by Tsunami. Coastal Engineering Journal. doi: 10.1142/S0578563416400179.
Kato, F., Y. Suwa, K. Watanabe, and S. Hatogai. 2012. Mechanisms of Coastal Dike Failure Induced by the Great East Japan Earthquake Tsunami. Coastal Engineering Proceedings 1:40. doi: 10.9753/icce.v33.structures.40.
Le, H., P. Moin, and J. Kim. 1997. Direct Numerical Simulation of Turbulent Flow over a Backward-Facing Step. Journal of Fluid Mechanics 330. doi: 10.1017/S0022112096003941.
Madsen, O. S., and W. D. Grant. 1976. Quantitative description of sediment transport by waves. Coastal Engineering.
Manenti, S., S. Sibilla, M. Gallati, G. Agate, and R. Guandalini. 2012. SPH Simulation of Sediment Flushing Induced by a Rapid Water Flow. Journal of Hydraulic Engineering 138:272–284. doi: 10.1061/(asce)hy.1943-7900.0000516.

McGovern, D. J., D. Todd, T. Rossetto, R. J. S. Whitehouse, J. Monaghan, and E. Gomes. 2019. Experimental observations of tsunami induced scour at onshore structures. Coastal Engineering 152:103505. doi: 10.1016/j.coastaleng.2019.103505.

Mikami, T., S. Matsuba, and T. Shibayama. 2014. Flow Geometry of Overflowing Tsunamis around Coastal Dykes. Coastal Engineering Proceedings 1:15. doi: 10.9753/icce.v34.currents.15.

Mikami, T., T. Shibayama, M. Esteban, T. Takabatake, R. Nakamura, Y. Nishida, H. Achiari, Rusli, A. G. Marzuki, M. F. H. Marzuki, J. Stolle, C. Krautwald, I. Robertson, R. Aránguiz, and K. Ohira. 2019. Field Survey of the 2018 Sulawesi Tsunami: Inundation and Run-up Heights and Damage to Coastal Communities. Pure and Applied Geophysics 176:3291–3304. doi: 10.1007/s00024-019-02258-5.

Mohr, O. 1914. Abhandlungen aus dem Gebiete der Technischen Mechanik. . Wilhelm Ernst und Sohn.

Moideen, R., M. R. Behera, A. Kamath, and H. Bihs. 2019. Effect of Girder Spacing and Depth on the Solitary Wave Impact on Coastal Bridge Deck for Different Airgaps. Journal of Marine Science and Engineering 7:140. doi: 10.3390/jmse7050140.

Nistor, I., D. Palermo, Y. Nouri, T. Murty, and M. Saatcioglu. 2009. Tsunami-Induced Forces on Structures. Pages 261–286 Handbook of Coastal and Ocean Engineering. doi: 10.1142/9789812819307_0011. . WORLD SCIENTIFIC.

Omira, R., G. G. Dogan, R. Hidayat, S. Husrin, G. Prasetya, A. Annunziato, C. Proietti, P. Probst, M. A. Paparo, M. Wronna, A. Zaytsev, P. Pronin, A. Giniyatullin, P. S. Putra, D. Hartanto, G. Ginanjar, W. Kongko, E. Pelinovsky, and A. C. Yalciner. 2019. The September 28th, 2018, Tsunami In Palu-Sulawesi, Indonesia: A Post-Event Field Survey. Pure and Applied Geophysics 176:1379–1395. doi: 10.1007/s00024-019-02145-z.

Palermo, D., I. Nistor, M. Saatcioglu, and A. Ghobarah. 2013. Impact and damage to structures during the 27 February 2010 Chile tsunami. Canadian Journal of Civil Engineering 40:750–758. doi: 10.1139/cjce-2012-0553.

Papadopoulos, G. A. 2016. Tsunamis in the European-Mediterranean Region. . Elsevier.

Prasetya, G. S., W. P. De Lange, and T. R. Healy. 2001. The Makassar Strait Tsunamigenic Region, Indonesia. Natural Hazards.

Putra, P. S., A. Aswan, K. A. Maryunani, E. Yulianto, and W. Kongko. 2019. Field Survey of the 2018 Sulawesi Tsunami Deposits. Pure and Applied Geophysics 176:2203–2213. doi: 10.1007/s00024-019-02181-9.

Qiu, Y., and H. B. Mason. 2019. Pore Water Pressure Response of Fully Saturated Soil Beds during Earthquake–Tsunami Multi-Hazards. Bulletin of the Seismological Society of America 109:1785–1796. doi: 10.1785/0120190031.

Ratha, D., and A. Sarkar. 2015. Analysis of flow over backward facing step with transition. Frontiers of Structural and Civil Engineering 9:71. doi: 10.1007/s11709-014-0270-x.

Rijn, L. C. van. 1984. Sediment transport, Part 1: Bed load transport. Journal of Hydraulic Engineering.

Rijn, L. C. van. 1993. Principles of sediment transport in rivers, estuaries and coastal seas. . Aqua Publications.

Robertson, I. 2014. Development of Tsunami Loading Expressions for Design of Coastal Infrastructure. IABSE Symposium Report. doi: 10.2749/222137814814068067.

Robertson, I., M. Esteban, J. Stolle, T. Takabatake, H. Mulchandani, T. Kijewski-Correa, D. Prevatt, D. Roueche, and K. Mosalam. 2019. StEER - PALU EARTHQUAKE AND TSUNAMI, SUWALESI, INDONESIA: FIELD ASSESSMENT TEAM 1 (FAT-1) EARLY ACCESS RECONNAISSANCE REPORT (EARR). doi: 10.17603/DS2JD7T. . Designsafe-CI.

Sassa, S., and T. Takagawa. 2018. Liquefied gravity flow-induced tsunami: first evidence and comparison from the 2018 Indonesia Sulawesi earthquake and tsunami disasters. Landslides:1–6.
Schendel, A., N. Goseberg, and T. Schlurmann. 2016. Erosion Stability of Wide-Graded Quarry-Stone Material under Unidirectional Current. Journal of Waterway, Port, Coastal, and Ocean Engineering 142:04015023. doi: 10.1061/(asce)ww.1943-5460.0000321.
Schendel, A., N. Goseberg, and T. Schlurmann. 2018. Influence of reversing currents on the erosion stability and bed degradation of widely graded grain material. International Journal of Sediment Research 33:68–83. doi: 10.1016/j.ijsrc.2017.07.002.
Seiffert, B., M. Hayatdavoodi, and R. C. Ertekin. 2014. Experiments and computations of solitary-wave forces on a coastal-bridge deck. Part I: Flat Plate. Coastal Engineering 88:194–209. doi: 10.1016/j.coastaleng.2014.01.005.
Seiffert, B. R., R. C. Ertekin, and I. N. Robertson. 2015. Wave loads on a coastal bridge deck and the role of entrapped air. Applied Ocean Research 53:91–106. doi: 10.1016/j.apor.2015.07.010.
Shields, A. 1936. Anwendung der Aehnlichkeitsmechanik und der Turbulenzforschung auf die Geschiebebewegung. . Berlin: Preußische Versuchsanstalt für Wasserbau.
Shuto, N., and K. Fujima. 2009. A short history of tsunami research and countermeasures in Japan. Proceedings of the Japan Academy. Series B, Physical and biological sciences 85:267–275. Retrieved from https://www.ncbi.nlm.nih.gov/pmc/articles/PMC3621565/.
Shvidchenko, A. B., G. Pender, and T. B. Hoey. 2001. Critical shear stress for incipient motion of sand/gravel streambeds. Water Resources Research 37:2273–2283. doi: 10.1029/2000wr000036.
Sumer, B., and J. Fredsoe. 2002. The Mechanics of Scour in the Marine Environment. doi: 10.1142/4942.
Takagi, H., M. Pratama, S. Kurobe, M. Esteban, R. Aranguiz, and K. Bowei. 2019. Analysis of generation and arrival time of landslide tsunami to Palu City due to the 2018 Sulawesi Earthquake. Landslides. doi: 10.1007/s10346-019-01166-y.
Takakura, R., and I. N. Robertson. 2010. Reducing Tsunami Bore Uplift Forces by Providing a Breakaway Panel. . University of Hawaii, Manoa.
Terzaghi, K. von. 1925. Erdbaumechanik auf bodenphysikalischer Grundlage.
Tonkin, P. S., M. Francis, and J. Bricker. 2013. Limits on Coastal Scour Depths due to Tsunami. Pages 671–678 Sixth China-Japan-US Trilateral Symposium on Lifeline Earthquake Engineering, May 28-June 1, 2013, Chengdu, China. doi: 10.1061/9780784413234.086.
Tonkin, S., H. Yeh, F. Kato, and S. Sato. 2003. Tsunami scour around a cylinder. Journal of Fluid Mechanics 496:165–192. doi: 10.1017/S0022112003006402.
Ulrich, T., S. Vater, E. H. Madden, J. Behrens, Y. van Dinther, I. van Zelst, E. J. Fielding, C. Liang, and A.-A. Gabriel. 2019. Coupled, Physics-Based Modeling Reveals Earthquake Displacements are Critical to the 2018 Palu, Sulawesi Tsunami. Pure and Applied Geophysics 176:4069–4109. doi: 10.1007/s00024-019-02290-5.
USACE. 2016. HEC-RAS - River Analysis System, Hydraulic Reference Manual Edition 5.0.
USGS. 2018. Earthquake Face and Statistics. U.S. Geological Survey.
Wang, F., S. Wu, and B. Huang. 2019. Flow structure and unsteady fluctuation for separation over a two-dimensional backward-facing step. Journal of Hydrodynamics. doi: 10.1007/s42241-019-0036-y.
Widiyanto, W., P. B. Santoso, S.-C. Hsiao, and R. T. Imananta. 2019. Post-event field survey of 28 September 2018 Sulawesi earthquake and tsunami. Natural Hazards and Earth System Sciences 19:2781–2794. doi: 10.5194/nhess-19-2781-2019.
Yeh, H., and B. Mason. 2014. Sediment response to tsunami loading: Mechanisms and estimates. Géotechnique 64:131–143. doi: 10.1680/geot.13.P.033.

Yeh, H., S. Sato, and Y. Tajima. 2013. The 11 March 2011 East Japan earthquake and tsunami: tsunami effects on coastal infrastructure and buildings. Pure and Applied Geophysics 170:1019–1031.
Yeh, H., S. Tonkin, E. Heller, P. Arduino, F. Kato, and S. Sato. 2004. Mechanisms of Scour Induced by Tsunami Runup. Proc. of Second International Conference on Scour and Erosion.
Zhao, E., K. Qu, and L. Mu. 2019. Numerical study of morphological response of the sandy bed after tsunami-like wave overtopping an impermeable seawall. Ocean Engineering 186:106076. doi: 10.1016/j.oceaneng.2019.05.058.
Del Zoppo, M., T. Rossetto, M. Di Ludovico, and A. Prota. 2019. Assessing the effect of tsunami-induced vertical loads on RC frames. Proceedings of 1st fib Italy YMG Symposium.